

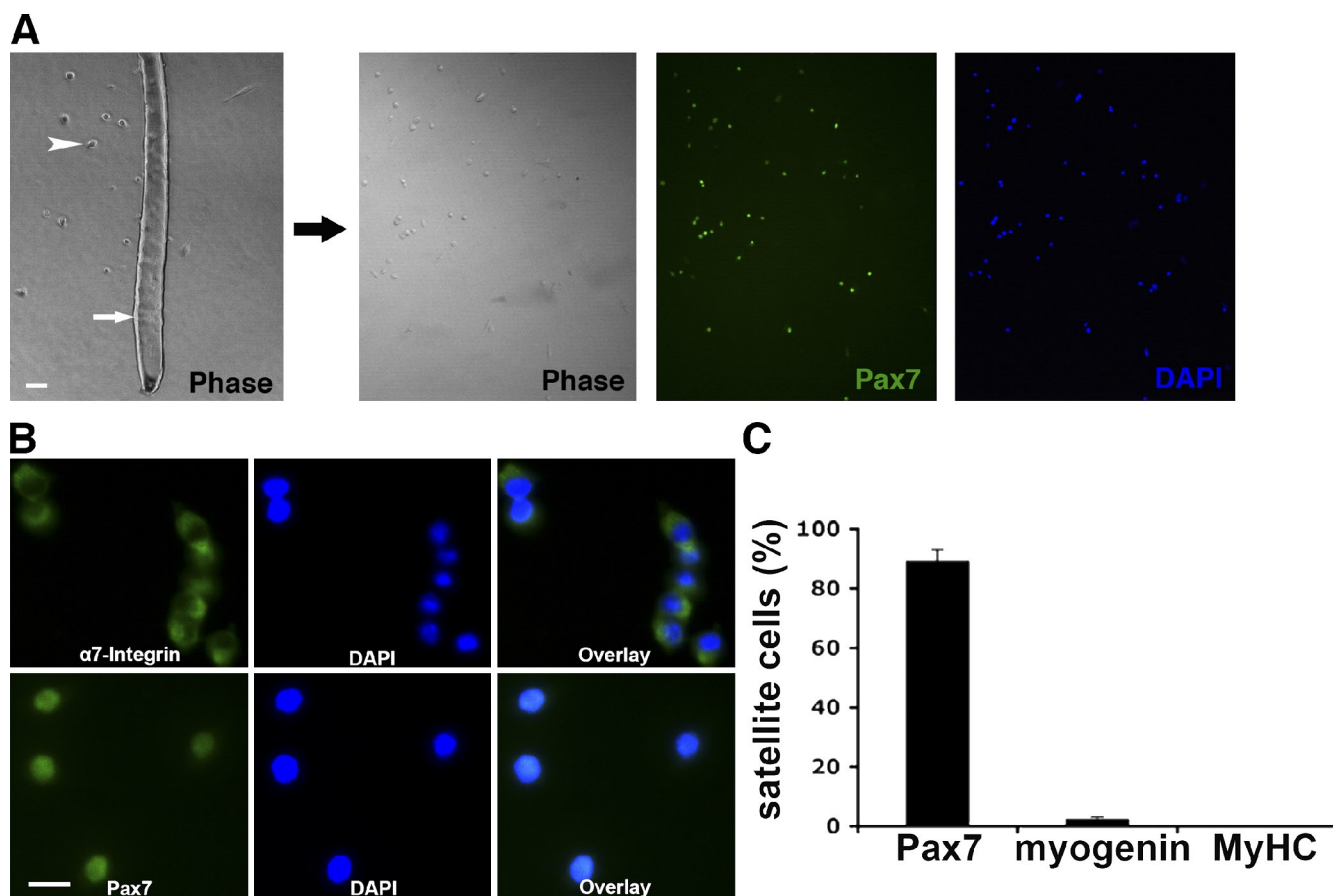
Chen et al., <http://www.jcb.org/cgi/content/full/jcb.200911036/DC1>

Figure S1. Isolation and phenotypic characterization of skeletal muscle satellite cells. (A) Isolation of satellite cells from single EDL myofibers. Brightfield image of a single myofiber isolated from the skeletal muscle of young adult mice. The arrow points to a single myofibers, and the arrowhead indicates a satellite cell. Satellite cells were immunostained positive for Pax7. DAPI-counterstained nuclei. Bar, 50 μ m. (B) Immunostaining of isolated satellite cells using antibodies against α 7-integrin and Pax7. DAPI-counterstained nuclei. Bar, 20 μ m. (C) Quantification of the distribution of cell population that express Pax7, myogenin, or MyHC, respectively, from isolated single myofiber-associated cells.

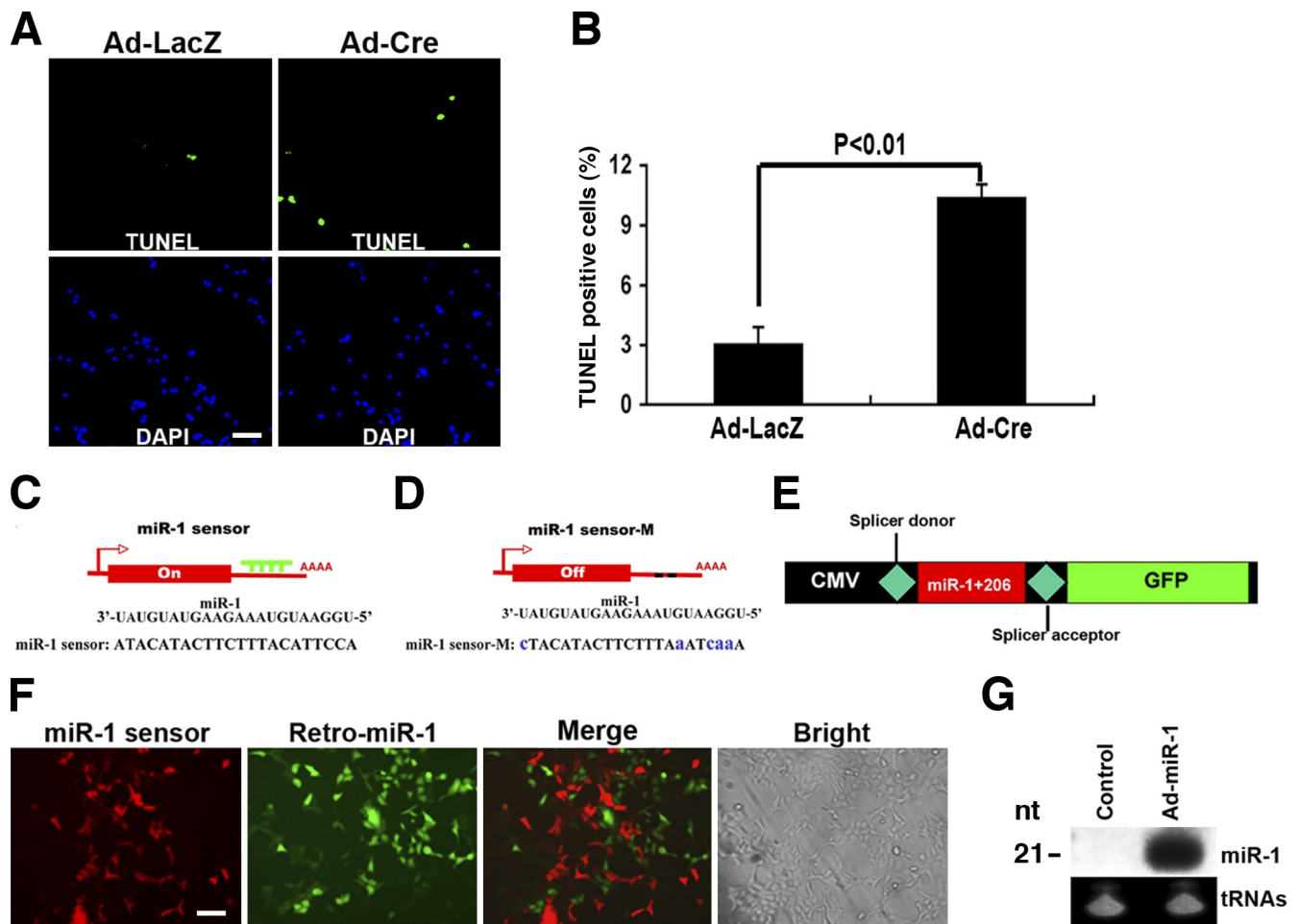


Figure S2. Dicer-depleted satellite cells exhibit higher rates of apoptosis in response to serum withdrawal. (A) Fluorescence-conjugated TUNEL analysis of *Dicer^{fllox/fllox}* satellite cells 48 h after infection with Ad-LacZ or Ad-Cre. (B) Quantification of TUNEL assay results in A. The TUNEL-positive cell percentage was calculated as the percentage of TUNEL-positive cells out of total number of cells indicated by DAPI-positive staining for each microscopic field. Error bars indicate SEM of 10 microscopic fields from three independent experiments. $P < 0.01$. (C and D) Scheme of the miR-1 sensor and mutated miR-1 sensor (miR-1 sensor M) constructs. (E) Diagram of the miR-1 and miR-206 expression strategy in which the precursor of the miRNAs, flanked by splicing donor and receptor, was cloned upstream of the GFP gene. Both miRNA and GFP genes were under the control of the cytomegalovirus (CMV) promoter. (F) Immunofluorescence of 293 cells infected with both adenoviral miR-1 sensor (red) and retroviral vector expressing miR-1 and miR-206 (green). (G) Northern blot analyses of miR-1 expression using RNA isolated from 293 cells infected with retroviral miR-1+206. tRNAs were used as a loading control. nt, nucleotide. Bars, 40 μ m.

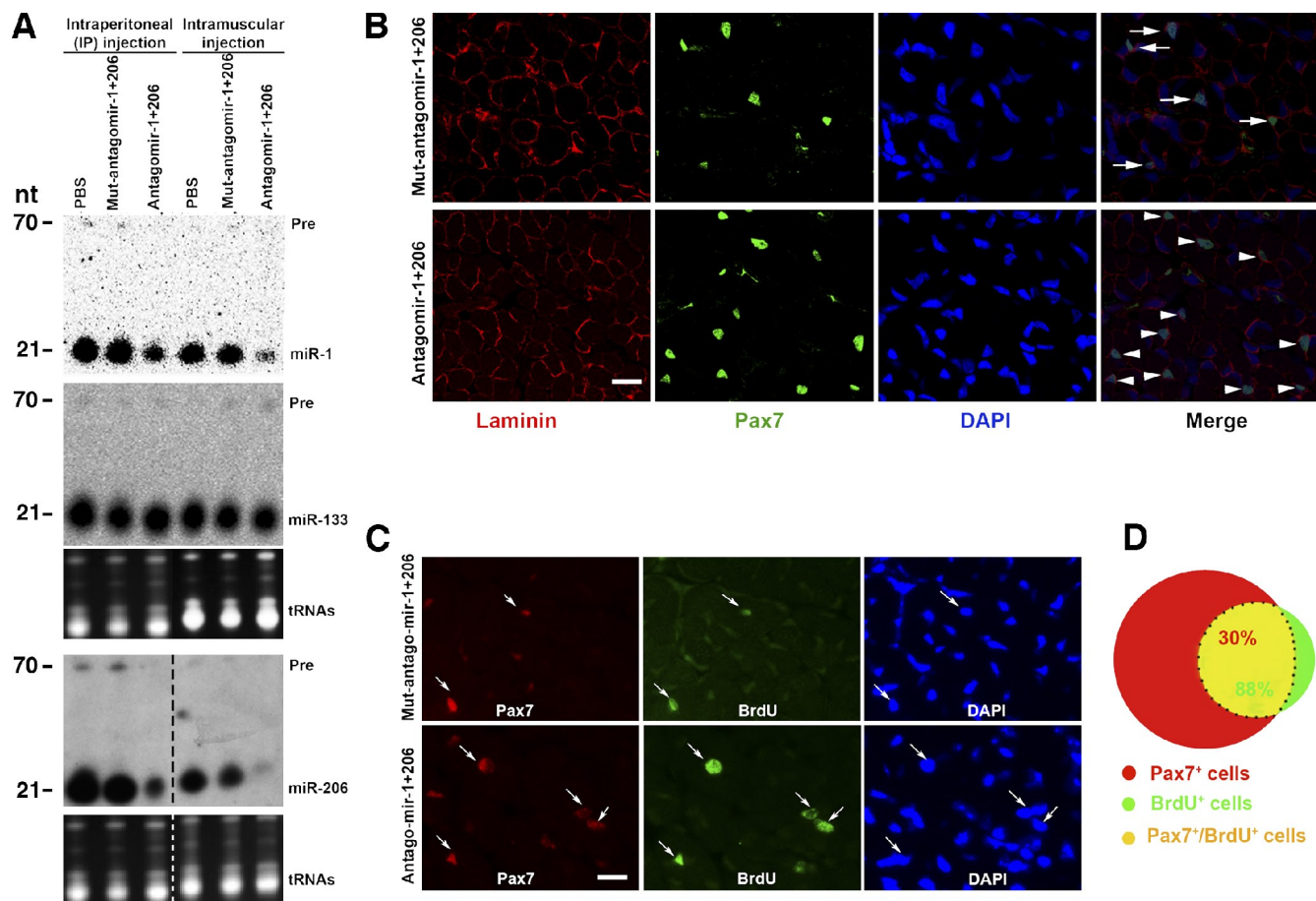


Figure S3. **Increased Pax7-positive satellite cells in antagomirs-1- and -206-treated skeletal muscle.** (A) Northern blot analyses of 10 µg total RNAs isolated from skeletal muscle 24 h after the last injection of mRNA antagomirs against miR-1 and miR-206 (antagomir-1+206). Results from both IP and intramuscular injection are shown. Muscle injected with PBS or mutated miR-1 and miR-206 antagomirs (mut-antagomir-1+206) were used as controls. tRNAs were used as a loading control. The dashed line indicates separated membranes. (B) Confocal microscopic images of skeletal muscle from antagomir-1+206- or mut-antagomir-1+206-treated mice. Anti-Pax7 antibody-labeled satellite cells (green). Laminin (red)-outlined cell surface and DAPI (blue)-counterstained nuclei. Arrows and arrowheads indicate Pax7-positive satellite cells. (C) Confocal microscopic images of skeletal muscle 4 h after BrdU labeling from postnatal mice treated with antagomir-1+206 or mut-antagomir-1+206 (serves as a control). Cell proliferation was determined by anti-BrdU antibody (green), satellite cells were marked by Pax7 (red), and DAPI (blue) counterstained nuclei. Arrows indicate Pax7 and BrdU double-positive cells. (D) Diagram of Pax7-positive and proliferating cells from experiments in B. Red, Pax7-positive cells; green, proliferating cells; yellow, Pax7 and BrdU double-positive cells. Note that 88% of BrdU-positive cells are satellite cells (Pax7 positive). Bars, 20 µm.

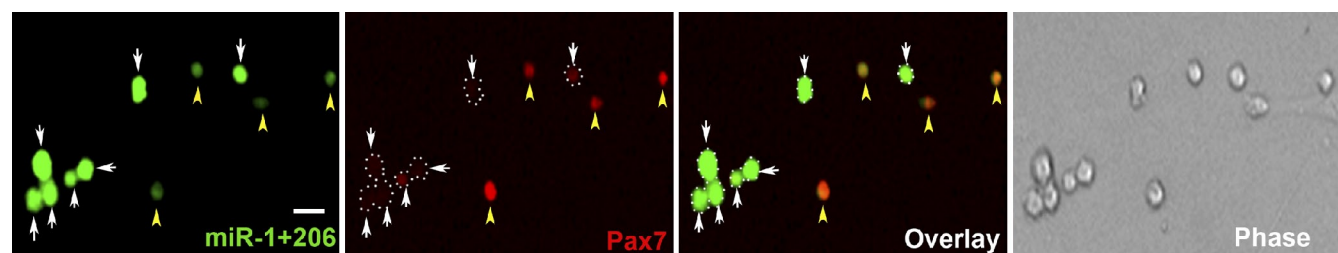


Figure S4. **miR-1 and miR-206 inhibit endogenous Pax7 protein expression.** Immunostaining of satellite cells using an antibody against Pax7. The satellite cells were infected with a retroviral vector expressing miR-1 and miR-206 or control. Note the mutually exclusive expression patterns of Pax7 (red; arrowheads) and miR1+206 (green; arrows). Dotted areas indicate satellite cells with high expression levels of miR-1 and miR-206. Bar, 20 µm.

